CHANGE DETECTION OF BUILDING MODELS FROM AERIAL IMAGES AND LIDAR DATA

Liang-Chien Chen [a,*], Li-Jer Lin [b], Hong-Kuei Cheng, [c] Shin-Hui Lee, [c]

[a] Center for Space and Remote Sensing Research, National Central University, No.300, Jhongda Rd., Jhongli City, Taoyuan County 320, Taiwan - lcchen@csrsr.ncu.edu.tw
[b] Department of Civil Engineering, National Central University, No.300, Jhongda Rd., Jhongli City, Taoyuan County 320, Taiwan - 973202088@cc.ncu.edu.tw
[c] CECI Engineering Consultants, Inc., 28th Floor, No. 185, Sec. 2, Sinhai Rd., Taipei City 10637, Taiwan - (tc561, shl)@ceci.com.tw

KEY WORDS: Change detection, Building, LIDAR, Image, Aerial

ABSTRACT:

Building models are built to provide three dimensional (3D) spatial information, which is needed for varieties of applications, such as city planning, construction of location-based services, and the like. However, three dimensional building models need to be updated from time to time. Rather than reconstructing building models for the entire area, it would be more effective to only revise the parts that have changed. In this study, we aim at finding changes with 3D building models. The proposed scheme comprises three steps, namely, (1) data registration, (2) change detection of three dimensional building models, and (3) detection of new building models. The first step performs data registration for multi-source data. The second step performs the rule-based change detection, it include examination of spectrum from aerial images, examination of height difference between building models and LIDAR points, and examination of linear features from aerial images. A double-threshold strategy is applied to cope with the highly sensitive thresholding often encountered when using the rule-based approach. In the third step, we detect the LIDAR point clouds in the new building areas by removing vegetation, ground and old building areas. We then use region growing to separate the LIDAR point clouds into different groups. Finally, we use boundary tracing to get the new building areas. Ground truth data are used for validation. The experimental results indicate that the double-threshold strategy improves the overall accuracy from 93.1% to 95.9%. To provide comprehensive observations, the different cases are scrutinized.

1. INTRODUCTION

A cyber city can be constructed which contains more spatial information than traditional two-dimensional topographic maps. This also provides the possibility to comprehensively integrate various types of 3D information. Three dimensional building models are one important part of a cyber city. Considering the rapidity of urban growth, a 3D geographic system is in need for updating the building models in the 3D information system. The effective revision of spatial data becomes important. Currently, change detection is usually done through spectral analysis of multi-temporal images. Nevertheless, building models also have three-dimensional information. So, we try to fuse the LIDAR data and aerial images for building model change detection. LIDAR data and aerial images have their own particular advantages and disadvantages in terms of horizontal and vertical accuracy. Compared with aerial images, LIDAR data provide more accurate height information but less accurate boundaries. Aerial images provide more extensive 2D information such as high resolution texture and color information. Although 3D height information can be estimated from one or several images by the use of several methods (such as stereo, shape from shading, comparison to LIDAR) the height information extracted from aerial images is still relatively less accurate. (Lee *et al.*, 2008).

Several studies of change detection using spectral imagery have been reported (Metternicht, 1999). Recently, a number of change detection methods using LIDAR data have been proposed. Murakami *et al.* (1999) used multi-temporal LIDAR data to produce Digital Surface Models (DSMs) for the detection of changes. Walter (2004) used LIDAR data for object-based classification and observation of land phenomena to determine the land-use category. There has been many studies using the vector maps (Knudsen and Olsen, 2003; Matikainen *et al.*, 2004), LIDAR data (Girardeau-Montau *et al.*, 2005; Murakami *et al.*, 1999), and aerial imagery (Jung, 2004) as the old data set. Some have used 3D building models as the old data set for this purpose (Huang, 2008).

2. METHODOLOGY

Since Lidar data and aerial images have unique advantages and disadvantages, it is natural to integrate those two data sets. In this paper, we aim to find the changed 3D building models using old building models with new LIDAR data and aerial imagery. It includes two parts in change detection. One is change detection of old buildings; the other is detection of new buildings. The workflow is shown in Fig 1.

* Corresponding author.

2.1 Data registration

First, we register the LIDAR data, aerial images and building models. The control points are measured and the mapping functions selected for registration of the three data sets to the same coordinate systems. There are two parts in this step, namely, planimetric registration and elevation registration. The image coordinate system is used as reference for planimetric registration, because the images provide high planimetric accuracy. The LIDAR coordinate system is used as reference for elevation registration, because the LIDAR data provide more accurate elevation. Planimetric registration note X and Y shifts on the plane. The elevation registration adjusts the shifts in the Z direction.

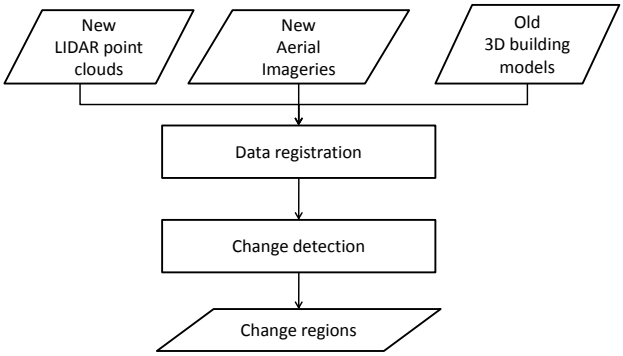

Figure 1. Workflow of the propose scheme

2.2 Change detection of 3D building models

In this part, we examine spectrum information from aerial images, height difference between the LIDAR points and the building models and linear features of the aerial images for detection of different types of change. First, we use the spectral information from the images. Here, NDVI is calculated to detect the area of vegetation for the exclusion of non-building areas. Second, we detect the LIDAR points which represent building roof planes, excluding the points on the wall and the convex points. Here, only points within the building boundaries are selected to be used for Delaunay triangulation. Third, facet orientation analysis is carried out for each triangle to detect those that might include wall points. Fourth, we calculate the center of the circumference for the triangle. The mean value and standard deviation of the elevation of the points in the circle are then calculated. Any point in a triangle with an elevation larger than two standard deviations is excluded. Fifth, we use equation 1 and the building model corner coordinates to calculate coplanarity parameters A, B, C. After this, the difference in height between the LIDAR points and the building models is calculated.

$$Z = AX + BY + C \quad (1)$$

The height differences (Δh) between the LIDAR points and building models comprise our major information about change. The workflow for calculation of height difference is shown in Fig 2. This detection process is done model by model. Since the height difference is, among others, the most important factor considered in this study, a double-threshold strategy on that is proposed to cope with the high sensitivity to thresholding often encountered with the rule-based approach. The double-threshold strategy distinguishes the obvious types of change first, so as to have more information and different thresholds to facilitate detection of the areas subject to further examination.

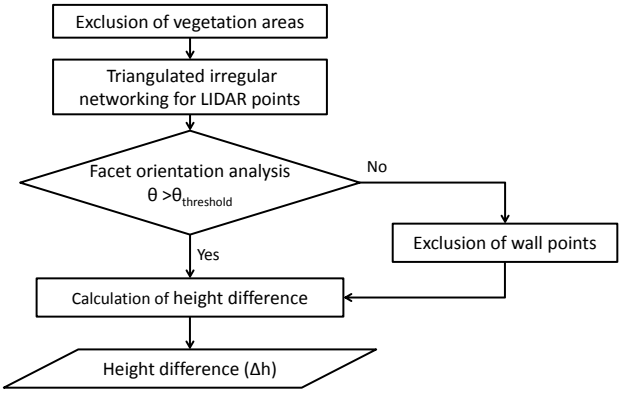

Fig 2. **C**alculation of height difference

Here, the line features in the aerial image give information that is used to refine the results. After this, we detect each building model to show the appropriate type of change. First, we set a double-threshold for height difference to discriminate between changed and unchanged points. The upper threshold is 3m and the low threshold is 1m. The 80% (δ_1) points in the building with height difference larger than upper threshold and the 80% (δ_2) points in the building with height difference smaller than low threshold are used to detect obvious changes and obvious unchanged in buildings. The data set between the double-threshold contain the areas subject to further examination. For the areas subject to further examination, additional information, line features from aerial images are added. The workflow for change detection is shown in Fig 3.

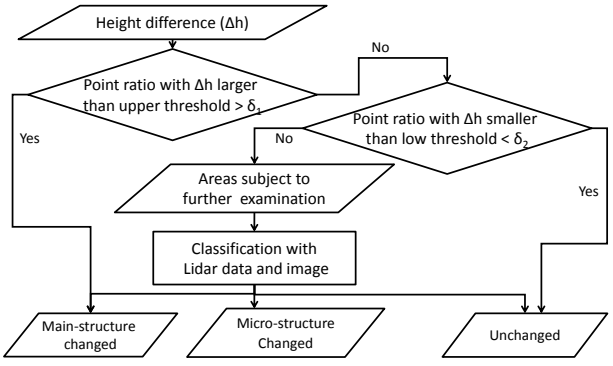

Fig 3. Change detection with double-thresholding

Line feature comparisons facilitate detection of the areas subject to further examination. The process for detection on areas subject to further examination is shown in Fig 4. Some parameters are to be set. The 50% (δ_3) points in the building with height difference larger than low threshold is used to detect the main-structure changed in buildings when the line feature comparisons are confirmed that there is no match. The 50% (δ_4) points in the building with height difference smaller than upper threshold is used to detect the unchanged in buildings when the line feature comparisons are confirmed that there is a match.

The 25m^2 (δ_5) of change area is used to detect the micro-structure changed in buildings.

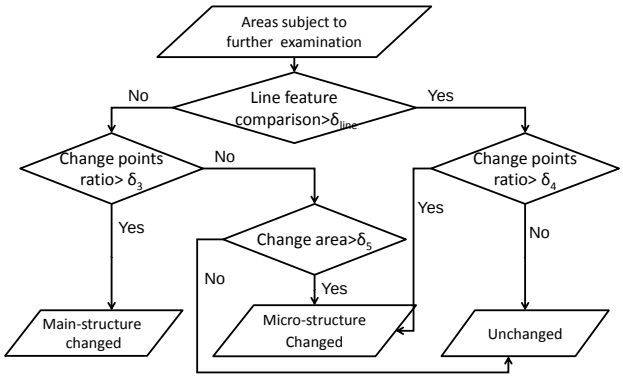

Fig 4. Change detection of areas subject to further examination

In the line feature comparisons, the aim is to compare building boundaries as they are shown in the building models and the aerial images. The idea is to extract the appropriate line features from the aerial images (i.e., the building boundaries) and compare them to the building boundaries in the models. The boundaries of the building models are first projected onto the aerial images to create the working area. Second, the line features are extracted from the aerial images by Canny edge detection and Hough transformation. Finally, the length ratio, angle and distance between model boundaries and line features are combined for line comparison (Lee *et al.*, 2008). By taking out the existing building boundaries, we can find whether there have been changes in the building models or not. The workflow for line feature comparisons procedures is shown in Fig 5.

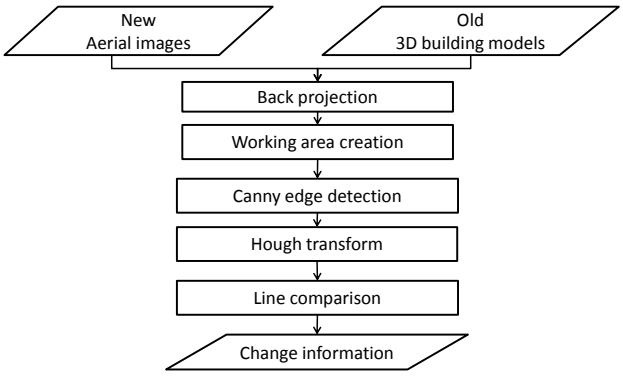

Fig 5. Workflow of line feature comparisons

2.3 Detection of new buildings

In this part, we detect the LIDAR point clouds in the new building areas by removing vegetation, ground and old building areas. First, we use NDVI to detect the area of vegetation. Second, we use the nDSM made from the LIDAR data to detect the area of ground. Finally, we use the old building models to detect the area of old buildings. After that, region growing is used to separate the LIDAR point clouds into different groups. The new building areas are detected after removing wall points and point groups with small area of the LIDAR point groups. Finally, we use the boundary tracing to get the boundaries of new building area. The work flow for detection of new buildings is shown in Fig 6.

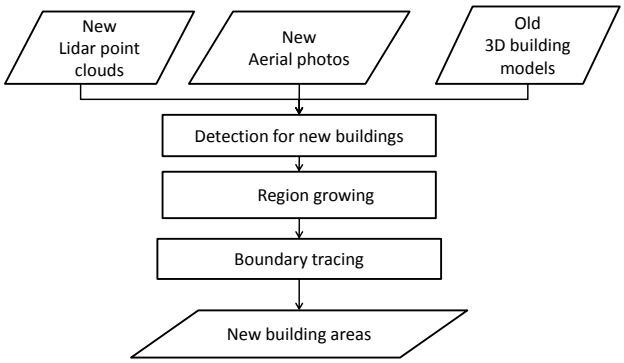

Fig 6. Workflow of detection of new buildings

3. EXPERIMENT AND RESULTS

The test site is located in Hsin-Chu City in Northern Taiwan. The old building models are polyhedral, built from a 2002 data set. It includes 492 building models. The aerial images were acquired using an UltraCam-D aerial digital camera with a 12cm resolution in June 2005. The LIDAR point clouds were acquired using a Leica ALS50 with a density of 1.7pts/m^2 also in June 2005. The test data information is shown in Table 7. Regarding the parameters set, the NDVI threshold for detection the area of vegetation is 0.3. The threshold of facet orientation analysis between triangle's normal vector and building model's normal vector is 20°. The upper and low thresholds of height difference are 3m and 1m, respectively. Table 8 lists the four point's ratio and one change area threshold with height difference in change detection. Table 9 lists the threshold for line comparisons.

Test data information	
Lidar data	
Density	1.7pts/m^2
Acquisition time	June 2005
Aerial images	
Resolution	12cm
Acquisition time	June 2005
Building models	
Form	polyhedral
reconstruction time	2002

Table 7. Data information

Threshold	value
Point ratio with Δh larger than upper threshold (δ_1)	80%
Point ratio with Δh smaller than low threshold (δ_2)	80%
Point ratio with Δh larger than low threshold (δ_3)	50%
Point ratio with Δh smaller than upper threshold (δ_4)	50%
Change area (δ_5)	25m^2

Table 8. Threshold with height difference in change detection

As shown in Fig 10, the detection results show the main-structure changes. The blue models show the correct detection results, the red models show the omission results. As shown in Fig 11, the detection results indicate micro-structure changes. The blue models show the correct detection results, the red models show the omission result. The detection results with no change are shown in Fig 12. The blue models show the correct detection results, the red models show the omission results.

Threshold	value
Length ratio	0.7
Angle	15°
Distance between lines	10 pixels

Table 9. Threshold for line comparison

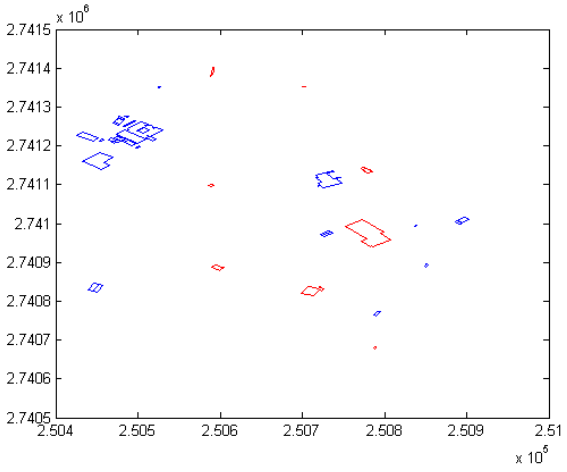

Fig 10. Detection result showing main-structure changes

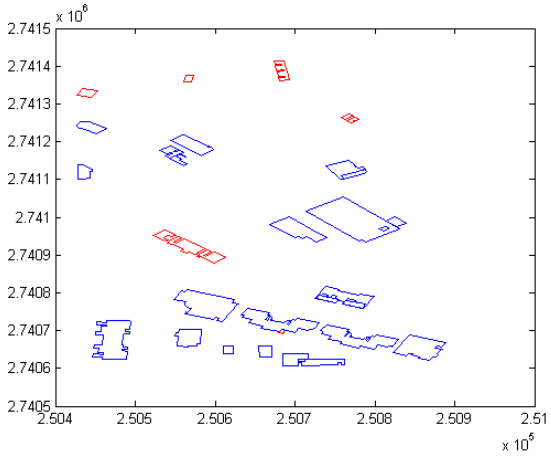

Fig 11. Detection results of micro-structure changes

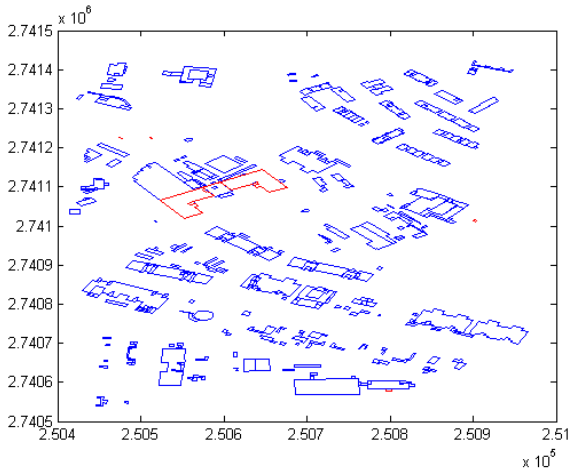

Fig 12. Detection result of no changed

Ground Truth \ TEST	Main-structure changed	Micro-structure changed	Unchanged	Total
Main-structure changed	**25**	**0**	**10**	**35**
Micro-structure changed	**0**	**24**	**1**	**25**
Unchanged	**13**	**10**	**409**	**432**
Total	**38**	**34**	**420**	**492**
		Diagonal total		**458**
Overall				**0.931**
Producer's	**0.714**	**0.960**	**0.947**	**0.874**
User's	**0.658**	**0.706**	**0.974**	**0.779**
Kappa				**0.714**

Table 13. Error matrix of detection with single-threshold strategy

Ground Truth \ TEST	Main-structure changed	Micro-structure changed	Unchanged	Total
Main-structure changed	**31**	**0**	**4**	**35**
Micro-structure changed	**0**	**24**	**1**	**25**
Unchanged	**8**	**7**	**417**	**432**
Total	**39**	**31**	**422**	**492**
		Diagonal total		**472**
Overall				**0.959**
Producer's	**0.886**	**0.960**	**0.965**	**0.937**
User's	**0.795**	**0.774**	**0.988**	**0.852**
Kappa				**0.829**

Table 14. Error matrix for detection with double-threshold strategy

After this, we used ground truth data for validation of the whole test site. The validation strategy for verification of the performance of double-threshold strategy includes two parts, i.e., double- threshold vs. single-threshold. The error matrix for the single threshold is shown in Table 13. The overall accuracy of the detection is 0.931. The producer's accuracy is 0.874, and the user's accuracy is 0.779. The error matrix for the double-threshold strategy is shown in Table 14. The overall accuracy of the detection is 0.959. The producer's accuracy is 0.937 and the user's accuracy is 0.852. The accuracy shows improvement with the double-threshold strategy.

To scrutinize the performance of the proposed method, two representative cases are discussed. These two cases explain why the detection failed. For the second part of the discussion, we look at two incorrect detections. The aerial images, LIDAR data and building models for case (a) and (b) are illustrated in Fig 15.

	(a)	(b)
Aerial Image		
Lidar points in the building model	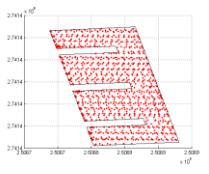	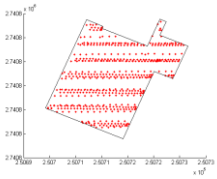
Building model	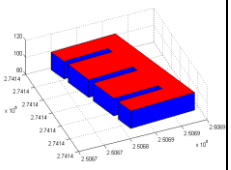	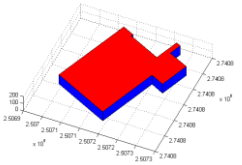

Fig 15. Incorrect detections case (a) and (b)

We observe that the ground truth data show no change for the two buildings in case (a) and (b). However, they have been classified as "changed". Explanations are given as follows. In case (a), it is an unchanged building that has been classified to micro-structure changes. The reason is that some of the LIDAR points on the wall were not excluded. Those points cause the incorrect detection. As shown in Fig 16, the blue points are the LIDAR points within the building polygons, the green points are the points removed after Delaunay triangulation. The red points are the changed points. Notice that the detection changed points are almost the points on the wall that should be excluded.

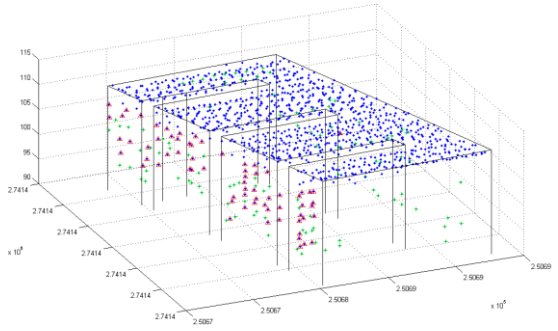

Fig 16. Changed points in case (a)

In case (b), it is an unchanged building that has been classified to main-structure changes. The reason is that the building roof has tiny roof variations. The variations cause some of the points detected as change points. Those points affect the detection. As shown in Fig 17, the blue points are the LIDAR points within the building polygons, the green points are the points removed after Delaunay triangulation. The red points are the changed points. Fig 17 shows the building roof has tiny variations.

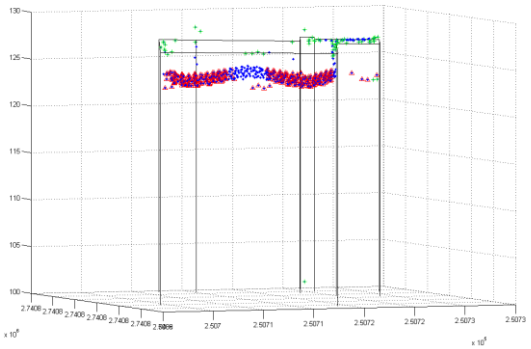

Fig 17. Changed points in case (b)

As shown in Fig 18, the detection results show the LIDAR point clouds in the new building areas by removing vegetation, ground and old building areas. As shown in Fig 18, these LIDAR points are discrete points, not regions. So, we use the region growing to separate the LIDAR point clouds into different groups. After that, we removed the wall points and point groups with small area of the LIDAR point groups. The result is shown in Fig 19. Finally, we use the boundary tracing to get the boundaries of new building area. The result is shown in Fig 20. The accuracy of new building detections is 100%. Nine new buildings in this test dataset are all detected by the proposed method. However, more test cases would be needed for comprehensive understanding.

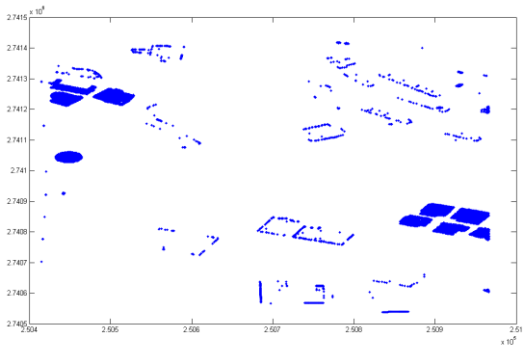

Fig 18. LIDAR point clouds detection result of new buildings

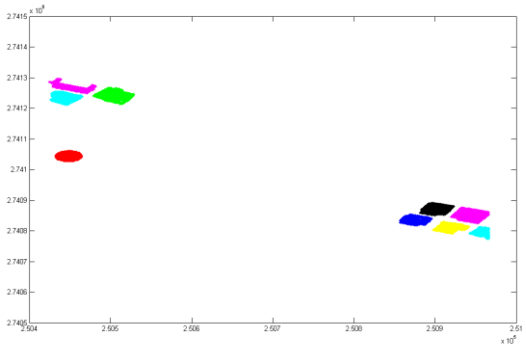

Fig 19. Detection result of new building areas

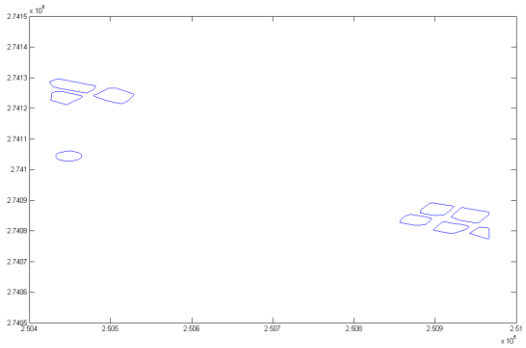

Fig 20. Result of boundary tracing

4. CONCLUSIONS

In this study, we have proposed a scheme for detection change by comparing old building models with new LIDAR and aerial imagery. The results include two parts. One is the change detection result of old buildings; the other is detection result of new building. Some change detection errors can be caused by the registration errors and tiny roof variations. If the building models of the roof are accurate and the registrations are accurate, the proposed method may achieve higher accuracy. The double-threshold strategy can also improve the accuracy. Although we only used line feature from the aerial images, texture information could also be used to refine the results. The accuracy of new building areas detection is 100%. However, there is only few new buildings in the test site, it should increase more test cases for comprehensive understanding.

REFERENCES

Girardeau-Montaut, D., Roux, M., Marc, R., and Thibault, G., 2005. Change Detection on Points Cloud Data Acquired with a Ground Laser Scanner, *International Archives of Photogrammetry, Remote Sensing and Spatial Information Sciences*, XXXVI (Pt. 3/W19):30-35.

Huang, C.Y., 2008. The Integration of Shape and Spectral Information for Change Detection of Building Models, Master. National Central University, Taiwan.

Jung, F., 2004. Detecting Building Changes from Multitemporal Aerial Stereopairs, *ISPRS Journal of Photogrammetry and Remote Sensing*, 58:187-201.

Knudsen, T. and Olsen, B.P., 2003. Automated Change Detection for Updates of Digital Map Databases, *Photogrammetric Engineering and Remote Sensing*, 69(11):1289-1296.

Lee, D.H., Lee, K.M. and Lee, S.U., 2008, Fusion of Lidar and Imagery for Reliable Building Extraction, *Photogrammetric Engineering and Remote Sensing*, 74(2):215-225.

Matikainen, L., Hyyppä, J., and Hyyppä, H., 2004. Automatic Detection of Changes from Laser Scanner and Aerial Image Data for Updating Building Maps, *International Archives of Photogrammetry, Remote sensing and Spatial Information Sciences*, XXXV (B2):434-439.

Metternicht, G., 1999. Change detection assessment using fuzzy sets and remotely sensed data: an application of topographic map revision, *ISPRS Journal of Photogrammetry & Remote Sensing*, 54:221-233.

Murakami, H., Nakagawa, K., Hasegawa, H., and Shibata, T., 1999. Change Detection of Buildings Using an Airborne Laser Scanner, *ISPRS Journal of Photogrammetry and Remote Sensing*, 54:148-152.

Walter, V., 2004. Object-based classification of remote sensing data for change detection, *ISPRS Journal of Photogrammetry & Remote Sensing*, 58:225-238.

ACKNOWLEDGMENTS

This investigation was partially supported by the National Science Council of Taiwan under Project No. NSC98-2622-E-008-003-CC2 and the CECI Engineering Consultants, Inc. under Project No.98923.